

## 브롬화된 부틸고무의 탈브롬화 및 이성질체화 메커니즘에 대한 연구

Yibo Wu, Wenli Guo<sup>†</sup>, Shuxin Li, Liangfa Gong, and Yuwei Shang

Department of Material Science and Engineering,  
Beijing Institute of Petrochemical Technology, Beijing, 102617, China  
(2009년 9월 29일 접수, 2009년 10월 15일 수정, 2009년 11월 19일 채택)

### Study on the Isomerization and Dehydrobromination Mechanism of Brominated Butyl Rubber

Yibo Wu, Wenli Guo<sup>†</sup>, Shuxin Li, Liangfa Gong, and Yuwei Shang

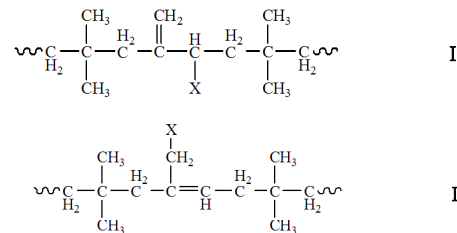
Department of Material Science and Engineering,  
Beijing Institute of Petrochemical Technology, Beijing, 102617, China  
(Received September 29, 2009; Revised October 15, 2009; Accepted November 19, 2009)

**Abstract:** Effects of reaction time and temperature on the isomerization and dehydrobromination reactions of brominated butyl rubber were investigated. The structural composition of brominated butyl rubber was determined by Fourier transform infrared spectroscopy (FT-IR) and proton nuclear magnetic resonance spectroscopy (<sup>1</sup>H-NMR). Density functional theory (DFT) was used to study on the isomerization and dehydrobromination mechanisms of model compounds. The geometries for model compounds of 3-bromo-5,5,7,7-tetramethyl-2(2',2',4',4'-tetramethyl)pentyl-1-octylene (3BrOE), 1-bromo-5,5,7,7-tetramethyl-2(2',2',4',4'-tetramethyl)pentyl-2-octylene (1Br2OE) and 5,5,7,7-tetramethyl-2(2',2',4',4'-tetramethyl)pentyl-1,3-octadiene (CD) had been optimized by using density functional theory at B3LYP/3-21G and B3LYP/6-31G levels. The predicted energy of 3BrOE lies higher than that of 1Br2OE which suggests that 1Br2OE configuration is more stable than the 3BrOE configuration. Compared with the energy barrier, the pathway of dehydrobromination is less competitive than that of isomerization. This is qualitatively consistent with the experimental results.

**Keywords:** brominated butyl rubber, isomerization, dehydrobromination, density functional theory.

### Introduction

It has been reported that brominated butyl rubbers are manufactured by adding molecular bromine to a solution of butyl rubber in a hydrocarbon solvent.<sup>1–3</sup> Accurate knowledge of the amount and types of unsaturation is important, where the major bromine-containing isomers vary significantly in the reactivity. Generally, the main structural formular for brominated butyl rubber is typically represented as structure I. In this structure, the double bond is external relative to the backbone of the polymer; The bromine atom is in a secondary allylic position. Gardner<sup>4</sup> disclosed another structural configuration for the brominated butyl rubber which is represented as structure II. In this structure, the Br atom is in a primary allylic position.



About the mechanism on halogenation of butyl rubber model compounds, Vukov<sup>5</sup> had suggested the classical electrophilic substitution mechanism in 1984. He has pointed out that the formation of the secondary allylic bromide configuration (structure I) partly results from the steric hindrance imposed by methyl group in the reaction of solution of butyl rubber with molecular bromine. Subsequently, some literatures reported that the structure I could be rearranged to II (I → II) or dissociated into HBr and conjugated diene (I → HBr + conjugated diene), when heated to 150 °C or above.<sup>6,7</sup>

In spite of the previous theoretical and experimental efforts

<sup>†</sup>To whom correspondence should be addressed.  
E-mail: gwenli@yahoo.cn

for the reactions of F or Cl with unsaturated hydrocarbons,<sup>8–10</sup> the kinetics and mechanisms of isomerization or dehydrobromination reactions in preparing brominated butyl rubber has not been investigated in detail in all previous experiments, and no report is found about the theoretical study on the title reaction. The objective of the present article is to investigate mechanisms of rearrangement and dehydrobromination reactions by quantum chemistry computation and laboratorial investigation. The theoretical study was based on density functional theory, a methodology that allowed for prediction of reaction mechanism.<sup>11,12</sup> Due to the complexity of the brominated butyl rubber phase, the construction of the initial model was based on the brominated isoprene unit of the backbone of polymer. The model compounds (3Br1OE: 3–Br–5,5,7,7–tetramethyl–2(2',2',4',4'–tetramethyl)pentyl–1–octylene and 1Br2OE: 1–Br–5,5,7,7–tetramethyl–2(2',2',4',4'–tetramethyl)pentyl–2–octylene) which is structurally similar to structure I and II are selected to investigate some properties.

## Experimental

**Materials.** Butyl rubber (unsaturation 1.8%, Bayer Chemical Co.) was chipped into pieces before dissolved in hexane. Fresh bromine (97%, Br), epoxidized soybean oil (99%) and hexane (99.99%) were used as received from Beijing Chemical Co.

**Preparation of Brominated Butyl Rubber.** Reactions were carried out in 1 L baffled glass reactor, equipped with a mechanical stirrer. The reaction flask was protected from direct sunlight to minimize light induced bromination. Butyl rubber was dissolved in hexane and transferred into the reaction vessel. Bromination was started by the injection of bromine solution. Reaction time was varied between 1 and 10 min. Reaction was terminated by addition of aqueous solution of sodium hydroxide, followed by the addition of stabilizers, and epoxidized soybean oil. The hexane solution was subsequently washed with distilled water and polymer was recovered by removing the solvent on a rotary evaporator and drying under vacuum at ambient temperature.

**Analysis.** FT–IR spectroscopy was performed on a Bruker Equinox 55 using KBr pellets as substrates. IR  $\delta\nu(\text{cm}^{-1})$ : 2975 ( $\text{H}_3\text{C}$ –); 1641 (C=C); 1363, 1389 ( $\text{H}_3\text{C}$ –); 1225 (C–C); 840 (C–H); 662 (C–Br).

$^1\text{H-NMR}$  ( $\text{CDCl}_3$ ) spectra were obtained at ambient temperature using a Bruker Avance 400 MHz Spectrometer.

**Computational Methods.** All calculations were carried out with the software package Gaussian 03. Geometry optimizations and frequency calculations were performed by the

density functional theory (DFT) Becke three–parameter combined with the Lee, Yang, and Parr correlation functional hybrid model (B3LYP)<sup>13,14</sup> using the 3–21 G and 6–31 G basis sets. Vibrational frequency calculations were used to determine whether a critical point was a minimum or a transition state: all positive frequencies for a minimum or one imaginary frequency (a first–order saddle point) for a transition state. Natural bond orbital (NBO) analysis was carried out at the B3LYP/3–21G level. Throughout the whole Letter, bond lengths were given in Å.

## Results and Discussion

**Theoretical Calculation.** We present the structure of the reactant, structure I and the product, structure II. The optimized geometries of model compounds (3Br1OE:3–

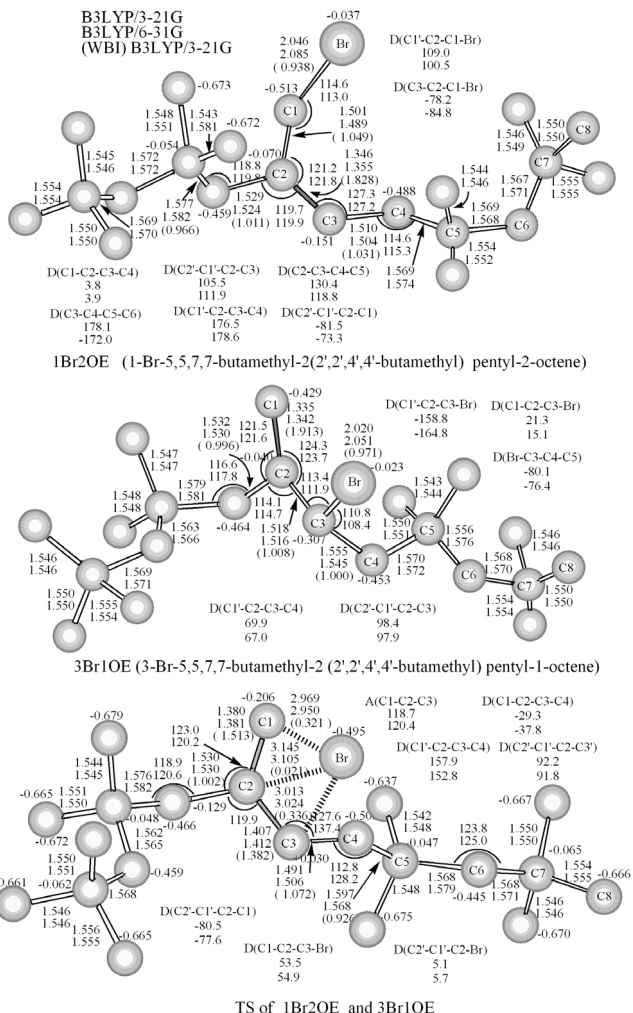


**Figure 1.** Optimized geometries of 1Br2OE, 3Br1OE, and the transition state (TS) of interconversion at the B3LYP/3–21G and B3LYP/6–31G levels. Wiberg bond indices (WBI) and atomic charges at B3LYP/3–21 G level.

$\text{Br}-5,5,7,7\text{-tetramethyl-}2(2',2',4',4'\text{-tetramethyl})\text{pentyl-}1\text{-octylene}$  and  $(1\text{Br}2\text{OE}:1-\text{Br}-5,5,7,7\text{-tetramethyl-}2(2',2',4',4'\text{-tetramethyl})\text{pentyl-}2\text{-octylene})$ , and the transition state (TS) between them were shown in Figure 1 respectively, along with the Wiberg bond indices (WBI) of bonding atoms and the natural charges, computed with density functional theory (DFT) at the B3LYP/3-21G and B3LYP/6-31G level. The mechanism of the dehydrohalogenation was discussed previously and the optimized geometry of the transition state ( $\text{TS}_{\text{di}}$ ) and conjugated diene configuration were shown in Figure 2. The calculated total energy and

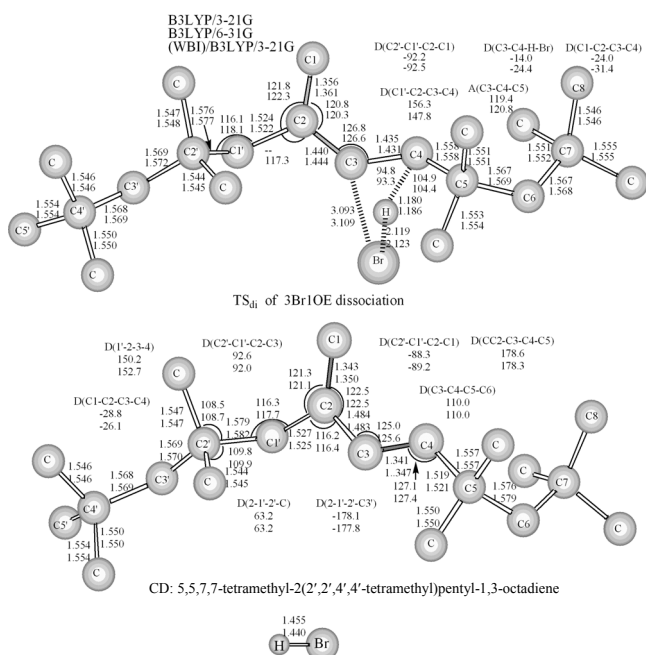


**Figure 2.** Optimized geometries of the transition state ( $\text{TS}_{\text{di}}$ ) of dissociation of 3Br1OE and the dissociation products: 5,5,7,7-tetramethyl-2(2',2',4',4'-tetramethyl)pentyl-1,3-octadiene and HBr at the B3LYP/3-21G and B3LYP/6-31G levels.

**Table 1. Molecular Properties of Different Species, Including Total Energies (E in hartree), Zero-Point Energies (ZPE in kcal/mol), the Lowest Harmonic Vibrational Frequency ( $v_1$  in  $\text{cm}^{-1}$ ), Dipole Moment (Dipole in Debye), and the Difference of Energies of the Highest Occupied Molecular Orbital (HO) and the Lowest Unoccupied Orbital (LU) (LU-HO in eV) with B3LYP Method**

Basis set	Species	E	ZPE	$v_1$	Dipole	LU-HO
3-21G	1Br2OE	-3382.28067	368.36	19.4 (<1)	1.736	5.596
	3Br1OE	-3382.27021	368.54	14.7 (<1)	2.105	6.569
	TS	-3382.19439	366.49	521.5i(6)	5.656	1.673
	$\text{TS}_{\text{di}}$	-3382.21082	364.74	605.8i(74.1)	6.681	1.798
	CD	-819.84922	359.25	11.1 (<1)	0.419	5.537
	HBr	-2562.38733	3.24	2267.1(9.8)	1.220	7.855
6-31G	1Br2OE	-3396.31179	368.76	27.9(<1)	2.026	5.252
	3Br1OE	-3396.29675	368.05	13.5(<1)	2.539	6.389
	TS	-3396.23671	366.67	458.3i(5.7)	6.085	1.788
	$\text{TS}_{\text{di}}$	-3396.24997	364.49	485.4i(111.4)	7.156	1.969
	CD	-824.10402	358.73	12.2(<1)	0.443	5.364
	HBr	-2572.16518	3.48	2431.7(9.0)	1.381	7.911

zero-point vibrational energies of model compounds (3Br1OE and 1Br2OE), and TS,  $\text{TS}_{\text{di}}$  were depicted in Table 1. The relative energies of isomers were listed in Table 2. By means of the interrelation among the reactants, transition states, and products as the corresponding relative energies, the schematic profiles of the energy barriers in isomerization and dehydrohalogenation reactions are depicted as shown in Figure 3.

**Isomerization.** From the relative energies of different species listed in Table 2 it can be seen that the 1Br2OE configuration is more stable than the 3Br1OE configuration by 6.74 and 8.73 kcal/mol (including the zero point energy (ZPE) correction) at B3LYP/3-21G and B3LYP/6-31 G levels, respectively. The optimized bond lengths, bond angles of transition state (TS) structure were depicted in Figure 1. At two levels of theory, the intrinsic reaction coordinates (IRC) were calculated from the transition states to identify these genuine transition states. According to the geometries as well as the high imaginary frequencies, they are tight transition states. At the B3LYP/6-31 G level, the only one imaginary vibrational frequency ( $458.3\text{i cm}^{-1}$ ) was obtained. We further noted that  $\text{Br}\cdots\text{C}1$  and  $\text{Br}\cdots\text{C}3$  distances of 3.013 Å and 2.969 Å, which were longer than corresponding  $\text{Br}-\text{C}3$  bond in 3Br1OE and  $\text{Br}-\text{C}1$  bond in 1Br2OE, respectively. So, the Br atom transferred was closer to the C1 atom. Moreover, the C1-C2 and C2-C3 bond lengths in transition state (TS) structure were similar and between

**Table 2. Calculated Relative Energies (kcal/mol) of Different Species with B3LYP Method (The ZPE-Corrected Results are Given in Parentheses)**

Basis set	1Br2OE	3Br1OE	TS	$\text{TS}_{\text{di}}$	CD+HBr
3-21G	0.0	6.57(6.74)	54.14 (52.27)	43.83(40.21)	27.69(21.81)
6-31G	0.0	9.44 (8.73)	47.11 (45.02)	38.79(34.52)	26.73(20.18)

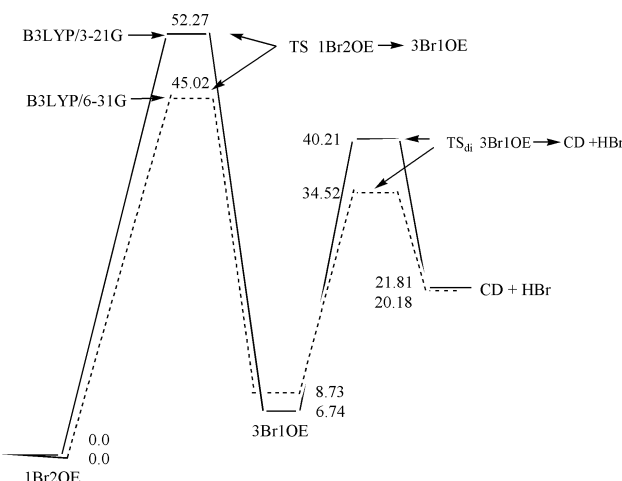


**Figure 3.** Relative energy profiles with respect to the most stable isomer 1Br2OE. Relative energies are in kcal mol<sup>-1</sup>.

those calculated for single (1.50 Å) and for double (1.33 Å) C=C bonds. The Wiberg bond indices (WBIs) between the adjacent atoms by NBO analyses demonstrated the same trend above. So the geometries of TS indicate that the isomerization of C=C double and formation new Br–C single bond occur simultaneously.

The bond angles and the dihedral angles on the main Br–isoprene units change largely in the interconversion of 3Br1OE into 1Br2OE. According to the present mechanism, the forward energy barrier of isomerization from 3Br1OE to 1Br2OE is about 45.5 and 36.3 kcal/mol at B3LYP/3–21G and B3LYP/6–31 G levels, and the reverse energy barrier is about 52.3 and 45 kcal/mol, which means that this isomerization reaction is easy to proceed at or above room temperature, and when the temperature increased, the lower energetically 1Br2OE species can be obtained mostly. Therefore, thermodynamic considerations may rule out the significance of pathway from 3Br1OE to 1Br2OE.

**Dehydrobromination.** The other important reaction pathway was the dehydrobromination via overcoming the transition state leading to conjugated 5,5,7,7-tetramethyl-2(2',2',4',4'-tetramethyl) pentyl-1,3-octadiene and HBr products. Figure 2 show the optimized geometry of the transition state (TS<sub>di</sub>) obtained for this process: C3–Br and C4–H bonds being elongated; the charged small negative Br being approached to the adjacent charged positive H atom, with the distance of H–Br attains 2.119, 2.123 Å. TS<sub>di</sub> transition state also has been characterized by the high imaginary frequency (605.8 i cm<sup>-1</sup> and 485.4 i cm<sup>-1</sup> at B3LYP/3–1G and B3LYP/6–21G level, respectively).

As shown in Figure 3, the energy barrier (33.5, 25.8 kcal/mol) of pathway from 3Br1OE to diene and HBr was higher than these in pathway from diene and HBr to 3Br1OE (18.4,

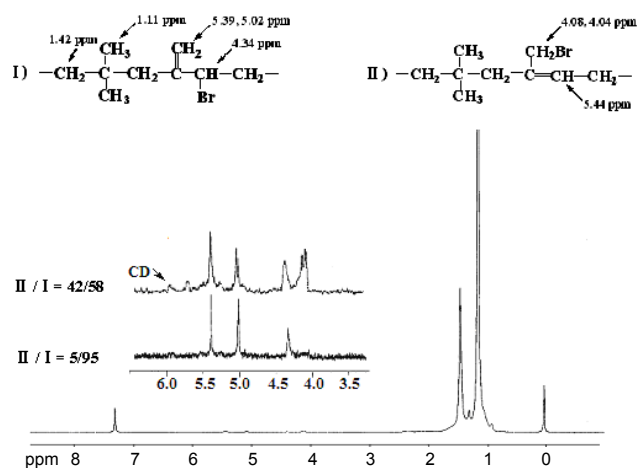


**Figure 4.** <sup>1</sup>H-NMR of brominated butyl rubber in CDCl<sub>3</sub>.

**Table 3. Effect of Reaction Time on Ratio of II/I and Bromine Content of Brominated Butyl Rubber**

Contact time(min)	1	2	3	5	6	7	8	9	10
II/I	5/95	21/79	31/69	35/65	42/58	47/53	47/53	48/52	50/50
Br content(%)	1.16	1.38	1.59	1.62	1.68	1.69	2.00	2.01	2.20

Conditions: 5% fresh bromine; 65 °C; 15 wt% polymer solution.

14.3 kcal/mol). So, pathway from 3Br1OE to conjugated diene (CD) + HBr should be less competitive than pathway from diene+HBr to 3Br1OE. Thus, compared with the isomerization reaction from 3Br1OE to 1Br2OE, the dehydrobromination of 3Br1OE should not be domination channel.

**Temperature Effect.** The chemical shift assignment of brominated butyl rubber is illustrated in Figure 4. Peak at 4.34 ppm is attributed to the proton on brominated carbon in structure I. While, peaks at 4.08 and 4.04 ppm are assigned to the protons on brominated carbon in structure II. According to the relative peak area ratios, the isomerization can be monitored. Comparing the ratio of 5/95 for II/I, peaks at 4.08 and 4.04 ppm became considerably sharper at the ratio of 48/52 for II/I. It was important to note that the content of conjugated diene (CD) structures (peak at 6.03 ppm) was very small and was close to negligible; this indicated the dehydrobromination reaction was not the domination channel. This was also in good agreement with our theory calculations.

The results of reaction time effect on ratio of II to I and bromine content of brominated butyl rubber were listed in Table 3. It was evident that the weight percent of combined bromine and the ratio of II to I increase with prolonging reaction time. At this temperature, combined bromine increased up to 2.2 wt% after 10 min. The longer the contact time, the more fractions of bromine are present in the structure II. Temperature dependence of the ratio of II

**Table 4. Effect of Temperature on Ratio of II/I and Bromine Content of Brominated Butyl Rubber**

Temperature(°C)	35	45	55	65	75	85
II/I	15/85	21/79	32/68	44/56	47/53	47/53
Bromine content(%)	0.85	0.87	0.86	0.95	1.21	1.30

Conditions : 2.5% fresh bromine; 15 wt% polymer solution, 5 min reaction time.

to I and bromine content was also illustrated by Table 4. Upon increasing the temperature from 35 to 85 °C, the ratio of II to I and the weight percent of combined bromine also increased. The experiments described above demonstrated that prolonging reaction time or increasing temperature could accelerate isomerization from I to II.

## Conclusions

Prolonging reaction time or increasing temperature can accelerate isomerization of brominated butyl rubber from structure I to structure II. The mechanisms of isomerization and dehydrobromination reaction have been studied theoretically by means of density functional theory. The energy of the optimized 3Br1OE (model of structure I) lies higher than that of 1Br2OE (model of structure II) which confirmed 1Br2OE configuration was more stable than the 3Br1OE configuration. The transition state (TS) between 3Br1OE and 1Br2OE configurations, and TS<sub>di</sub> for 3Br1OE dissociated into conjugated diene+HBr has been successfully found. The activation energies (E<sub>a</sub>) of isomerization and dissociation have been calculated. Compared with the energy barrier of dehydrobromination reaction, the isomerization was dominant channel.

**Acknowledgment:** This work was supported by Beijing Municipal Project for Developing Advanced Human Resources for Higher Education and Beijing Institute of Petrochemical Technology Foundation for the Youth (Grant No. 09-02; No.07-05).

## References

1. C. Y. Chu, K. N. Watson, and R. Vukov, *Rubber Chem. Technol.*, **60**, 636(1987).
2. I. J. Gardner, U.S. Patent 3,293,323(1966).
3. J. Gardner, U.S. Patent 4,288,575(1979).
4. I. J. Gardner, J. V. Fusco, and F. P. Baldwin, U.S. Patent 4,681,921(1984).
5. R. Vukov, *Rubber Chem. Technol.*, **57**, 275(1984).
6. R. Vukov, *ACS Rubber Division Meeting*, 1983.
7. G. Kaszas, *Rubber Chem. Technol.*, **73**, 356(1999).
8. P. Bran and J. A. Sordo, *J. Am. Chem. Soc.*, **123**, 10348 (2001).
9. J. Stutz, M. J. Ezell, and A. A. Ezell, *J. Phys. Chem. A*, **102**, 8510 (1998).
10. J. L. Li, C. Y. Geng, and X. R. Huang, *J. Chem. Theory Comput.*, **2**, 1551 (2006).
11. M. Boronat, P. Viruela, and A. Corma, *J. Phys. Chem. A*, **102**, 982 (1998).
12. C. Y. Lin and J. J. Ho, *J. Phys. Chem. A*, **106**, 4137(2002).
13. A. D. Becke, *J. Chem. Phys.*, **98**, 5648 (1993).
14. C. Lee, W. Yang, and R. G. Parr, *Phys. Rev. B*, **37**, 785 (1988).